Available online at www.sciencedirect.com
ScienceDirect
Journal of Power Sources 161 (2006) 601–605
JOURNAL OF POWER SOURCES
www.elsevier.com/locate/jpowsour

Short communication

Effects of synthesis conditions on the structural and electrochemical properties of layered $Li[Ni_{1/3}Co_{1/3}Mn_{1/3}]O_2$ cathode material via the hydroxide co-precipitation method LIB SCITECH

Xufang Luo [a], Xianyou Wang [a,*], Li Liao [a], Ximin Wang [a], Sergio Gamboa [b], P.J. Sebastian [b]

[a] *College of Chemistry, Xiangtan University, Hunan 411105, PR China*
[b] *Solar-Hydrogen-Fuel Cell Group, CIE-UNAM, Temixco 62580, Morelos, Mexico*

Received 17 February 2006; accepted 18 March 2006
Available online 12 June 2006

Abstract

The uniform layered $Li[Ni_{1/3}Co_{1/3}Mn_{1/3}]O_2$ cathode material for lithium ion batteries was prepared by using $(Ni_{1/3}Co_{1/3}Mn_{1/3})(OH)_2$ synthesized by a liquid phase co-precipitation method as precursor. The effects of calcination temperature and time on the structural and electrochemical properties of the $Li[Ni_{1/3}Co_{1/3}Mn_{1/3}]O_2$ were systemically studied. XRD results revealed that the optimal prepared conditions of the layered $Li[Ni_{1/3}Co_{1/3}Mn_{1/3}]O_2$ were 850 °C for 18 h. Electrochemical measurement showed that the sample prepared under the above conditions has the highest initial discharge capacity of 162.1 mAh g^{-1} and the smallest irreversible capacity loss of 9.2% as well as stable cycling performance at a constant current density of 16 mA g^{-1} between 3 and 4.3 V versus Li at room temperature.

Keywords: Lithium ion battery; $Li[Ni_{1/3}Co_{1/3}Mn_{1/3}]O_2$; Hydroxide co-precipitation; Structure characteristics; Electrochemical properties

1. Introduction

Recently, $Li[Ni_{1/3}Co_{1/3}Mn_{1/3}]O_2$ as a special case among the $Li[Ni_xCo_{1-2x}Mn_x]O_2$ series where x is 1/3 has attracted a great deal of interest in the investigation of cathode materials for lithium ion batteries to replace the presently popular $LiCoO_2$ because the combination of Ni, Co, Mn can provide advantages such as stable cycling performance, good thermal stability and excellent rate capability [1–5]. It has a typical hexagonal α-$NaFeO_2$ structure with a space group of $R\bar{3}m$, the valence of Ni, Co and Mn in the compound are 2+, 3+ and 4+, respectively [6], only divalent Ni and trivalent Co are involved in the electrochemical processes through $Ni^{2+/4+}$ and $Co^{3+/4+}$ redox couples [7,8]. Tetravalent Mn, on the other hand, has a configuration of empty $3de_g$ orbitals in octahedral coordination so that it is electrochemically inactive. However, Mn plays an essential role in supporting the host structure during Li^+ de-/intercalation. It was reported that the rechargeable capacity of $Li[Ni_{1/3}Co_{1/3}Mn_{1/3}]O_2$ was 160 mAh g^{-1} when the cell operated at 2.5–4.4 V and more than 200 mAh g^{-1} in the voltage range of 2.8–4.6 V [3,9] and it is considered to be one of the best candidates for a positive electrode material for hybrid electric vehicle (HEV) power source system by Amine et al. [10]. However, the synthesis of homogenous $Li[Ni_{1/3}Co_{1/3}Mn_{1/3}]O_2$ is not easy, so selecting a suitable preparation method is important to obtain phase-pure final products. Many researchers have reported that employing coprecipitation to prepare metal hydroxide would be the best choice because the method essentially gives phase-pure oxide products [11–15]. Meanwhile, we can find that the heat-treatment of the precursor is very important to obtain $Li[Ni_{1/3}Co_{1/3}Mn_{1/3}]O_2$ with excellent properties. In this paper, $Li[Ni_{1/3}Co_{1/3}Mn_{1/3}]O_2$ was prepared by mixing uniform co-precipitated metal hydroxide, $(Ni_{1/3}Co_{1/3}Mn_{1/3})(OH)_2$ with 5% excess $LiOH{\cdot}H_2O$ followed by heat-treatment. The effects of the calcination temperature and time on the structural and electrochemical properties of the $Li[Ni_{1/3}Co_{1/3}Mn_{1/3}]O_2$ were studied in detail.

2. Experimental

In order to prepare a homogenous $(Ni_{1/3}Co_{1/3}Mn_{1/3})(OH)_2$ precursor, we applied hydroxide co-precipitation method

* Corresponding author. Tel.: +86 732 8293043; fax: +86 732 8292282.
E-mail address: wxianyou@yahoo.com (X. Wang).

0378-7753/$ – see front matter © 2006 Elsevier B.V. All rights reserved.
doi:10.1016/j.jpowsour.2006.03.090

as we previously reported [16]. An aqueous solution of $NiSO_4{\cdot}6H_2O$, $CoSO_4{\cdot}7H_2O$ and $MnSO_4{\cdot}H_2O$ (cationic ratio of Ni:Co:Mn = 1:1:1) with a concentration of 2 mol L^{-1} was precipitated by adding NaOH solution (aq.) of 2 mol L^{-1} and a desired amount of NH_4OH solution (aq.) separately under argon atmosphere along with continued stirring. The solution was maintained at 50 °C for 24 h and the pH was controlled to 10–11. Then, the spherical precursor was filtered, washed and dried in a vacuum at 50–60 °C overnight. The transition metal composition of the precursor was determined by atomic absorption spectroscopy (AAS). The obtained precursor powder was mixed with 5% excess $LiOH{\cdot}H_2O$ (excess amount of Li salts was used to compensate for possible Li loss during the calcinations) thoroughly using a ball mill and the powder was pressed into pellets. The pellets were initially heated to 480 °C for 5 h and then 650 °C for 9 h. The pellets were remade and subsequently calcined at 700–1000 °C for 18 h in air to obtain $Li[Ni_{1/3}Co_{1/3}Mn_{1/3}]O_2$.

Powder X-ray diffraction was carried out using a Cu Kα radiation of Rigaku D/max 2550 diffractometer. Silicon powder was used as an internal standard for the calculation of lattice parameters.

The cathode was prepared by mixing the active material with carbon black and PTFE in a weight ratio of 75:15:10. The mixture was pressed onto a stainless steel mesh used as the current collector and dried under vacuum at 120 °C for 24 h. The laboratory pouch cells consisting of the cathode, the lithium foil as an anode and 1 M $LiPF_6$-EC/DMC (1:1 in volume) as an electrolyte were assembled in an argon-filled glove box. Cycle tests were performed on the cells between 3 and 4.3 V at 0.1 C of a constant current at 30 °C with a BTS-51800 Neware Battery Testing System. (160 mA g^{-1} was assumed to be 1 C rate).

3. Results and discussion

The obtained brown colored powder from the hydroxide co-precipitation process was used as a precursor, the Ni/Co/Mn ratio in the precursor was determined to 0.33:0.34:0.33 by atomic absorption spectroscopy (AAS), which is almost the same as the design value. Fig. 1 shows the XRD patterns of the precursor $(Ni_{1/3}Co_{1/3}Mn_{1/3})(OH)_2$ and the mid-product of $Li[Ni_{1/3}Co_{1/3}Mn_{1/3}]O_2$. The X-ray diffraction pattern of the precursor (Fig. 1a) shows broad integrated lines and can be attributed to the mixture of transition metal (TM = Ni, Co, Mn) hydroxides. It can be seen from the XRD pattern of the mixture of the precursor and $LiOH{\cdot}H_2O$ (Fig. 1b) that there appeared several new diffraction peaks compared to the precursor (Fig. 1a). The XRD spectra recorded for the mixture heated to 480 °C for 5 h revealed the formation of the well-crystallized compound during the heating process (shown in Fig. 1c). However, in Fig. 1d, the sample which continued to be heated at 650 °C for 9 h appeared to have the characteristic of a layered structure to a certain extent though the diffraction peaks were slightly broad.

Fig. 2 illustrates the powder X-ray diffraction patterns of the samples calcined at different temperatures, such as 700, 800, 850, 900 and 1000 °C, respectively. Hereafter, the materials synthesized at 700, 800, 850, 900 and 1000 °C were

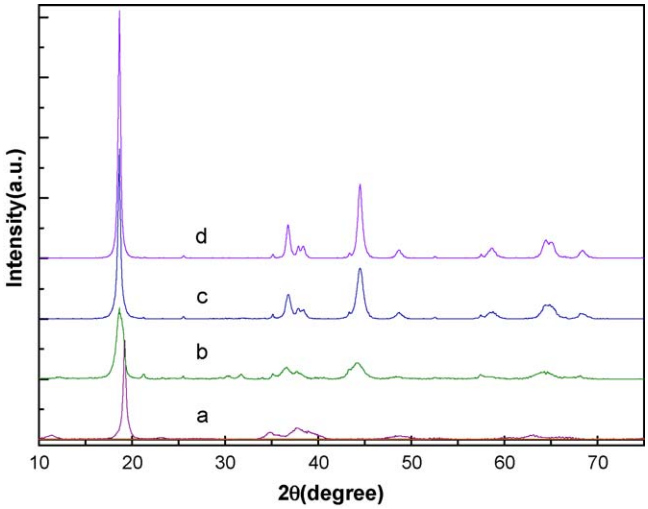

Fig. 1. X-ray diffraction pattern of the precursor and mid-product of the $Li[Ni_{1/3}Co_{1/3}Mn_{1/3}]O_2$ powder. (a) $(Ni_{1/3}Co_{1/3}Mn_{1/3})(OH)_2$ precursor; (b) precursor mixed with $LiOH.H_2O$; (c) 480 °C heated for 5 h; (d) 650 °C heated for 9 h.

referred as S70, S80, S85, S90 and S100. All the samples can be indexed to the hexagonal α-$NaFeO_2$ structure (space group: $R\bar{3}m$) without any impurity peaks. As being seen in Fig. 2, the splits in the (0 0 6)/(1 0 2) and (1 0 8)/(1 1 0) doublets observed in all the XRD patterns, indicating that the layered $Li[Ni_{1/3}Co_{1/3}Mn_{1/3}]O_2$ cathode material has been successfully synthesized at all the calcination temperature in this experiment though S70 and S100 showed slightly broader diffraction lines than those of the others.

The lattice parameters and other structural parameters calculated based on XRD results for $Li[Ni_{1/3}Co_{1/3}Mn_{1/3}]O_2$ are summarized in Table 1. Some researchers [17,18] used the high integrated intensity ratio of the I_{003}/I_{104} to indicate the cation mixing of the layered structure. Generally, when $I_{003}/I_{104} > 1.2$, the cation mixing is small with good layered structure. The I_{003}/I_{104} values of all the samples in this work are larger than 1.2,

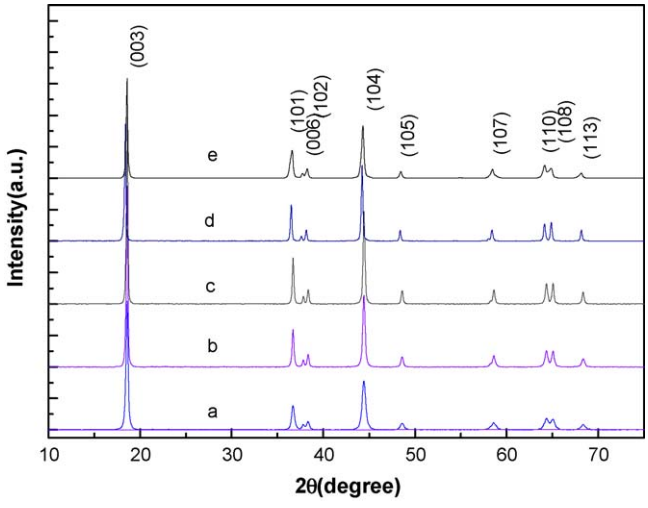

Fig. 2. X-ray diffraction pattern of the $Li[Ni_{1/3}Co_{1/3}Mn_{1/3}]O_2$ powder synthesized at various temperatures for 18 h. (a) 700 °C; (b) 800 °C; (c) 850 °C; (d) 900 °C; (e) 1000 °C.

Table 1
Calculated structure parameters for $Li[Ni_{1/3}Co_{1/3}Mn_{1/3}]O_2$ synthesized at various temperatures for 18 h

T (°C)	a (Å)	c (Å)	c/a	Volume (Å^3)	I_{003}/I_{104}	$R=(I_{102}+I_{006})/I_{101}$
700	2.862	14.235	4.974	100.96	1.35	0.5321
800	2.861	14.230	4.974	100.85	1.71	0.4786
850	2.862	14.229	4.972	100.91	1.73	0.4565
900	2.861	14.232	4.974	100.89	1.54	0.5034
1000	2.868	14.266	4.974	101.81	1.31	0.5066

indicating no undesirable cation mixing takes place. As shown in Table 1, with increasing calcination temperature from 700 to 900 °C, the lattice parameter, a, which is related to average metal-metal intra-slab distance, the lattice parameter, c, which is correlated to the average metal-metal inter-slab distance, the trigonal distortion, c/a, and the cell volume V underwent no apparent change. The lattice parameters are in good agreement with the literature [6,9,21]. While for S100, the lattice parameters a, c and V increase distinctly while the c/a ratio is virtually unchanged. These results indicate that the hexagonal ordering does not change with calcination temperature. In addition, Dahn et al. [19,20] believed that the R-factor ($R=(I_{102}+I_{006})/I_{101}$) was an indicator of hexagonal ordering, the lower the R-value, the better the hexagonal ordering. It can been seen from Table 1 that S85 has the lowest R-value of 0.4565, indicating the best hexagonal ordering.

In order to further study the influence of the calcination temperature on the electrochemical performance of $Li[Ni_{1/3}Co_{1/3}Mn_{1/3}]O_2$, the test cells were operated at a constant current density of 16 mA g^{-1} between 3 and 4.3 V versus Li at room temperature. Fig. 3 shows the initial charge/discharge curves of the $Li[Ni_{1/3}Co_{1/3}Mn_{1/3}]O_2$ powder synthesized at various temperatures for 18 h and Fig. 4 shows cycling performance of all the samples up to 20 cycles. As seen from the Figs. 3 and 4, all cells showed quite smooth and monotonous charge/discharge curves. On charging at 16 mA g^{-1}, the voltage suddenly increased to about 3.7 V and then held at 3.7–3.85 V until the charge capacity reached about 105 mAh g^{-1}, which could be attributed to the Ni^{2+}/Ni^{4+} redox reaction occurred in this region [3]. On further charging, the voltage curves monotonously increased to 4.3 V, which was similar to that observed by Ohzuku et al. [1]. Charge–discharge capacities and capacity retention ratios of all the samples are tabulated in Table 2. Although S70 has lower crystallinity than the other

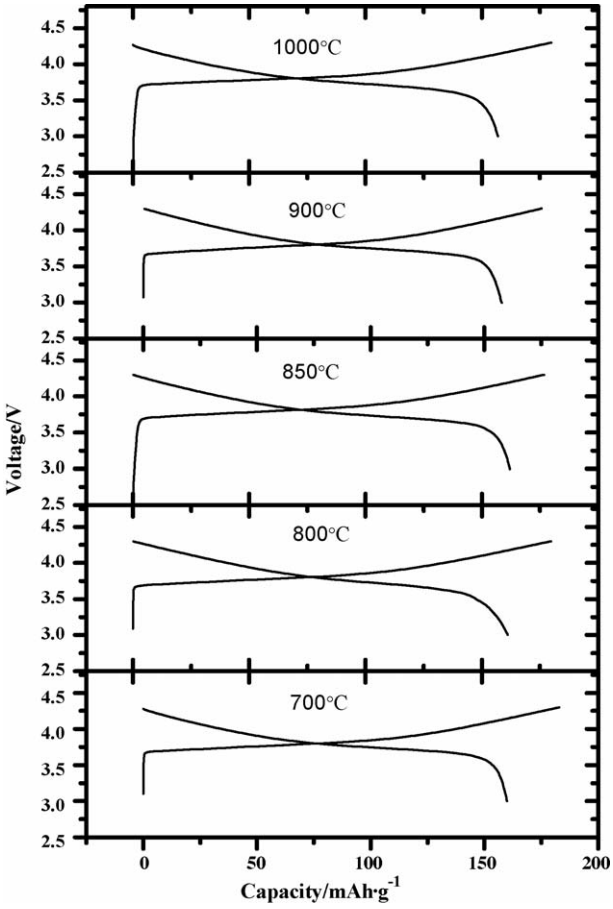

Fig. 3. The initial charge–discharge profiles of the synthesized $Li[Ni_{1/3}Co_{1/3}Mn_{1/3}]O_2$ (3–4.3 V) operated at 16 mA g^{-1} at 30 °C.

samples, it shows the highest charge capacity of 182.9 mAh g^{-1} and discharge capacity of 159.9 mAh g^{-1} in the first cycle, for which the efficiency corresponds to 85.6%. The discharge capacities of 161.2, 162.1, 157.5 and 156.9 mAh g^{-1} were obtained at the first cycle for S80, S85, S90 and S100, respectively. Furthermore, the irreversible capacity loss (IRC) of S70, S80, S90 and S100 were 14.4%, 11.4%, 11.2% and 14.6%, respectively. The smallest IRC of 9.2% was also obtained by S85. All samples have excellent cyclic performance. The reversible capacity after 20 cycles was 150.0 mAh g^{-1} (93.8% of the initial discharge capacity), 158.9 mAh g^{-1} (98.6% of the initial discharge capacity), 160.8 mAh g^{-1} (99.2% of the initial discharge capacity), 155.8 mAh g^{-1} (98.9% of the initial discharge capacity)

Table 2
Charge–discharge capacity of $Li[Ni_{1/3}Co_{1/3}Mn_{1/3}]O_2$ synthesized at various temperatures for 18 h

T (°C)	First charge capacity (mAh g^{-1})	First discharge capacity (mAh g^{-1})	Irreversible capacity loss (mAh g^{-1})	First discharge efficiency (%)	20th discharge capacity (mAh g^{-1})	20th capacity retention (%)
700	182.9	159.9	23.0	85.6	150.0	93.8
800	179.6	161.2	18.4	88.6	158.9	98.6
850	176.9	162.1	14.8	91.8	160.8	99.2
900	175.1	157.5	17.6	88.8	155.8	98.9
1000	179.9	156.9	23.0	85.4	151.6	96.6

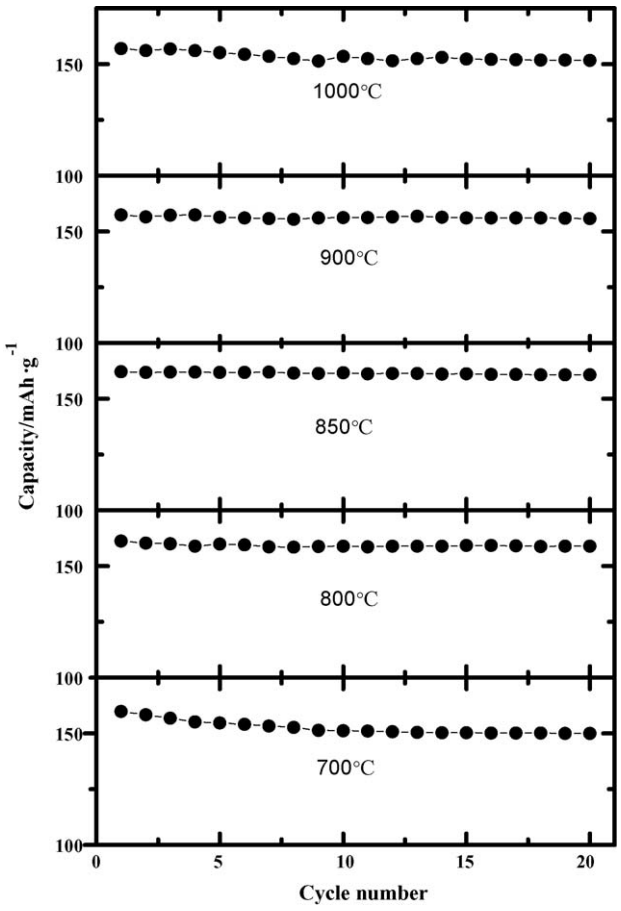

Fig. 4. Discharge capacities as a function of cycle number of the synthesized $Li[Ni_{1/3}Co_{1/3}Mn_{1/3}]O_2$ (3–4.3 V) operated at 16 mA g^{-1} at 30 °C.

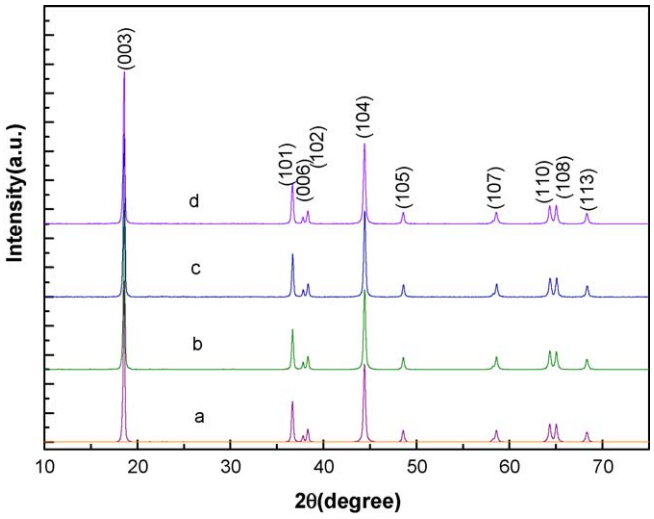

Fig. 5. X-ray diffraction pattern of the $Li[Ni_{1/3}Co_{1/3}Mn_{1/3}]O_2$ powder synthesized at 850 °C for different time. (a) 6 h; (b) 12 h; (c) 18 h; (d) 24 h.

Table 3
Calculated structure parameters for $Li[Ni_{1/3}Co_{1/3}Mn_{1/3}]O_2$ synthesized at 850 °C for different time

t (h)	a(Å)	c(Å)	c/a	volume (Å^3)	I_{003}/I_{104}	$R=(I_{102}+I_{006})/I_{101}$
6	2.862	14.233	4.973	100.99	1.58	0.5006
12	2.863	14.235	4.972	101.05	1.68	0.4774
18	2.862	14.229	4.972	100.91	1.73	0.4565
24	2.862	14.236	4.974	101.01	1.66	0.4786

and 151.6 mAh g^{-1} (96.6% of the initial discharge capacity) for S70, S80, S85, S90 and S100, respectively. These results are consistent with the XRD results in which the S85 has the highest I_{003}/I_{104} ratio of 1.73 and the lowest R-value of 0.4565 while the S70 has the highest R-value of 0.5321. As mentioned above, it can be concluded that $Li[Ni_{1/3}Co_{1/3}Mn_{1/3}]O_2$ reported in this paper has good electrochemical performance for the application as the cathode material of lithium ion batteries, and it can be considered that 850 °C is the best synthetic temperature of $Li[Ni_{1/3}Co_{1/3}Mn_{1/3}]O_2$ for using $(Ni_{1/3}Co_{1/3}Mn_{1/3})(OH)_2$ prepared by liquid phase co-precipitation method as precursor.

The influence of calcination time on the structural and electrochemical properties of $Li[Ni_{1/3}Co_{1/3}Mn_{1/3}]O_2$ was also investigated. Fig. 5 shows the X-ray diffraction patterns of the samples calcined at 850 °C for different time in air, viz., 6, 12, 18, 24 h. Hereafter, the materials synthesized at 6, 12, 18, 24 h were referred as T6, T12, T18 and T24, respectively. The lattice parameters and other structural parameters calculated for $Li[Ni_{1/3}Co_{1/3}Mn_{1/3}]O_2$ synthesized at different time are summarized in Table 3. The layered structure of the materials was confirmed by the clear splitting of the hexagonal doublet (0 0 6)/(1 0 2) and (1 0 8)/(1 1 0) as shown in Fig. 5. It can be seen from Table 3 that with increasing calcination time, the calculated lattice parameters a, c, c/a and unit cell volume V showed no obvious change. It is clear from above results that the hexagonal ordering does not change with calcination time. Table 4 shows the charge–discharge capacities and capacity retention ratios of $Li[Ni_{1/3}Co_{1/3}Mn_{1/3}]O_2$ calcined at 850 °C for different time in air. The first discharge capacities of T6, T12, T18 and T24 were 155.4, 159.6, 162.1 and 161.9 mAh g^{-1} and the cor-

Table 4
Charge–discharge capacity of $Li[Ni_{1/3}Co_{1/3}Mn_{1/3}]O_2$ synthesized at 850 °C for different time

t (h)	First charge capacity (mAh g^{-1})	First discharge capacity (mAh g^{-1})	Irreversible capacity loss (mAh g^{-1})	First discharge efficiency (%)	20th discharge capacity (mAh g^{-1})	20th capacity retention (%)
6	172.8	155.4	17.4	89.9	149.7	96.3
12	175.0	159.6	15.4	91.2	157.4	98.6
18	176.9	162.1	14.8	91.8	160.8	99.2
24	179.2	161.9	17.3	90.3	159.9	98.8

responding efficiencies were 89.9%, 91.2%, 91.8% and 90.3%, respectively. The capacity retention ratios of all samples were above 96% by the 20th cycle. Similarly, the best electrochemical property was obtained for T18 and so 18 h is the optimal calcination time for preparing $Li[Ni_{1/3}Co_{1/3}Mn_{1/3}]O_2$.

4. Conclusions

Well-ordered layered $Li[Ni_{1/3}Co_{1/3}Mn_{1/3}]O_2$ powder was successfully prepared by mixing uniform co-precipitated metal hydroxide, $(Ni_{1/3}Co_{1/3}Mn_{1/3})(OH)_2$ with 5% excess $LiOH{\cdot}H_2O$ under different calcination temperatures. The XRD results revealed that the I_{003}/I_{104} values of all the samples in this work are larger than 1.2 indicating no undesirable cation mixing takes place. Based upon the results of the electrochemical experiments, we concluded that the ideal synthesized conditions were 850 °C for 18 h. The layered $Li[Ni_{1/3}Co_{1/3}Mn_{1/3}]O_2$ material prepared under the optimal conditions has the highest I_{003}/I_{104} ratio of 1.73 and the lowest *R*-value of 0.4565, which shows the highest initial discharge capacity of 162.1 mAh g^{-1} (3–4.3 V, 0.1C) and the smallest irreversible capacity loss of 9.2%, as well as good cycle performance.

Acknowledgements

This work was financially supported by the Key Project of Department of Science and Technology of Hunan Province under the grant No. 05GK2015, the Key Project of Department of Education of Hunan Province under the grant No. 04A054, and the Key Project of Ministry of Education of China under the grant No. 205109.

References

[1] T. Ohzuku, Y. Makimura, Chem. Lett. 7 (2001) 642–643.
[2] I. Belharouak, Y.K. Sun, J. Liu, K. Amine, J. Power Sources 123 (2003) 247–252.
[3] D.C. Li, T. Muta, L.Q. Zhang, M. Yoshio, H. Noguchi, J. Power Sources 132 (2004) 150–155.
[4] J.M. Kim, H.T. Chung, Electrochim. Acta 49 (2004) 937–944.
[5] J. Choi, A. Manthiram, J. Electrochem. Soc. 152 (2005) A1714–A1718.
[6] T.H. Cho, S.M. Park, M. Yoshi, T. Hirai, Y. Hideshima, J. Power Sources 142 (2005) 306–312.
[7] K.M. Shaju, G.V. Subba Rao, B.V.R. Chowdari, Electrochim. Acta 48 (2002) 145–151.
[8] M.G. Kim, H.J. Shin, J.H. Kim, S.H. Park, Y.K. Sun, J. Electrochem. Soc. 152 (2005) A1320–A1328.
[9] N. Yabuuchi, T. Ohzuku, J. Power Sources 119–121 (2003) 171–174.
[10] G. Henriksen, K. Amine, J. Liu, P. Nelson, 204th Meeting of The Electrochemical Society, Orlando, 12–16 October, 2003, Abstract 255.
[11] C. Storey, I. Kargina, Y. Grincourt, I.J. Davidson, Y.C. Yoo, D.Y. Seung, J. Power Sources 97–98 (2001) 541–544.
[12] Z. Lu, D.D. MacNeil, J.R. Dahn, Electrochem. Solid State Lett. 4 (2001) A200–A203.
[13] S.H. Kang, K. Amine, J. Power Sources 119–121 (2003) 150–155.
[14] S. Jouanneau, K.W. Eberman, L.J. Krause, J.R. Dahn, J. Electrochem. Soc. 150 (2003) A1637–A1642.
[15] M.H. Lee, Y.J. Kang, S.T. Myung, Y.K. Sun, Electrochim. Acta 50 (2004) 939–948.
[16] X.F. Luo, X.Y. Wang, L. Liao, S. Gamboa, P.J. Sebastian, J. Power Sources, 2005, in press.
[17] Y.Gao, M. Yakovleva, H.H. Wang, J.F. Engel, U.S. Patent, 6620400, 2003.
[18] Z.L. Liu, A.S. Yu, J.Y. Lee, J. Power Sources 81–82 (1999) 416–419.
[19] J.R. Dahn, U. von Sacken, C.A. Michal, Solid State Ionics 44 (1990) 87–97.
[20] J.N. Reimers, E. Rossen, C.D. Jones, J.R. Dahn, Solid State Ionics 61 (1993) 335–344.
[21] S. Patoux, M.M. Doeff, Electrochem. Commun. 6 (2004) 767–772.